The 2009 IEEE/RSJ International Conference on
Intelligent Robots and Systems
October 11-15, 2009 St. Louis, USA

Toward Human-Like Walking Pattern Generator

Kensuke Harada, Kanako Miura, Mitsuharu Morisawa, Kenji Kaneko,
Shin'ichiro Nakaoka, Fumio Kanehiro, Tokuo Tsuji, and Shuuji Kajita

***Abstract*— In this paper, we generate the biped gait of a humanoid robot that looks like a human's one. To generate the human like motion, we first capture walking motion of a human. Then, we analyze the captured data and obtain several information such as the relationship between the step length and waist height etc. We consider applying these informations to the real humanoid robot. Also, when the human walks, the sway of the waist is smaller than most of the humanoid robot's one. By compensating the angular momentum of the robot and by modifying the ZMP trajectory, we show that sway of the robot's waist can be smaller. We show the effectiveness of the proposed method through simulation and experimental results.**

I. INTRODUCTION

Through the humanoid research, we aim to develop a humanoid robot that can work like a human in our daily life. To realize this goal, we first have to develop a humanoid robot that looks like a human. Then, this robot has to behave like a human and perform a task as a human can do. Recently, although there are a lot of works on the motion generation of a humanoid robot, the number of research on humanoid robots to generate a human-like motion is not large. On the other hand, this research focuses on the biped gait of a humanoid robot and is a first step on realizing the human-like walking motion based on the captured data of human motion.

Fig.1 shows the walking motion of a humanoid robot and a human. To generate a human-like biped gait of a humanoid robot, we can assume two approaches. The arrow (1) in Fig.1 shows the first approach where we start from the walking-pattern generator of a humanoid robot, and then modify the parameters of it such that the generated motion becomes as close as to a human's one. On the other hand, the arrow (2) shows the second one where we start from the captured data of a human motion, and then modify the captured motion so as to apply it to a humanoid robot. Among these two approaches, we focus on the first approach and consider realizing the human-like biped gait of a humanoid robot. To adjust the parameters of the walking-pattern generator, we use the captured data of a human's gait.

By using the walking-pattern generator of a humanoid robot, we can generate several walking motion having several step length, walking cycle time, and walking direction. This means that, to generate the human-like walking motion based on the captured data of human's motion, it is not enough to use a single captured data. Hence, we consider recording multiple captured data having several walking parameters.

The authors are with Intelligent Systems Research Institute, National Institute of Advanced Industrial Science and Technology
kensuke.harada@aist.go.jp

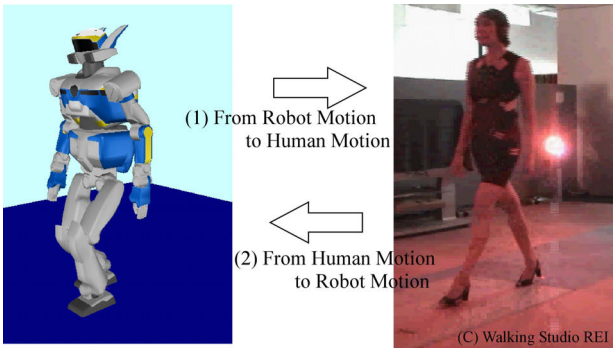

Fig. 1. Two Approaches on Generating Human Like Motion

After capturing multiple walking motions, we analyze the captured data and extract the relationship between each walking parameters. For example, we obtain the relationship between the vertical motion of the waist and the step length.

Most of the walking parameters can be obtained by using multiple captured data of human's motion. However, the horizontal motion of the waist cannot be determined by using the captured motion since it has to be determined by solving the ordinary differential equation for given ZMP trajectory. We show that the sway of the robot's waist is larger than the human's one if we solve the ordinary differential equation without considering the effect of the angular momentum. Also, we show that, by modifying the ZMP trajectory by referring the human's one, the sway of the waist can be further reduced.

The rest of this paper is organized as follows; after showing the related works in Section 2, we show the overview of the motion capture and the walking pattern generation in Section 3. In Section 4, we analyze the human motion capture. In Section 5, we analyze the sway of the waist. After showing the implementation issue in Section6, we show simulation and experimental results in Section 7.

II. RELATED WORKS

Several humanoid robots have been developed, including [13], [14], [15]. The following three approaches have been used to generate human-like motion for these robots:

a) Methods based on motion capture: Widely used in computer animation, these methods generate the motion of digital actors by stiching together pieces of captured human motion. Many techniques have been proposed, including one that is interactive [4], one that is constraint-based [5], and one that combines different captured motions for each limb [6]. A similar technique was even used to quantify, with a statistical

TABLE I
A SET OF CAPTURED DATA

#	Desired Step length [m]	Desired Cycle Time [s]	No. of Steps
1	0.15	1.0	24
2	0.3	0.75	12
3	0.3	1.25	13
4	0.45	Not Imposed	8
5	0.45	1.0	7
6	0.45	1.5	5
7	0.6	Not Imposed	8
8	0.6	1.5	5
9	0.6	2.0	4

model, what it means for human motion to be natural [3]. This approach has also been applied to humanoid robots [2], [1], [7]. These method can be classified as the method shown as the arrow (2) in Fig.1.

b) Methods based on optimization: Rather than copy human motion, these methods generate motion that is optimal with respect to a particular objective function. A number of objective functions have been proposed, including minimization of hand jerk [8], [10], minimization of the change of joint torque [9], and minimization of joint torque itself [11]. In [11], the gradient of the objective function was computed analytically, with application to a planar model of a humanoid. It has also been observed that angular momentum about the CoG is highly regulated in human walking motion [12], although this quantity has not been used previously as an objective function to generate natural humanoid motion.

c) Methods based on control: These methods use an onboard control strategy to achieve natural motion. One strategy is based on tracking linear and angular momentum [16]. Another is based on achieving a hierarchy of task-level objectives and postural constraints using an operational space forumulation [17]. In fact, our work could be used to define a set of appropriate postural constraints to be used by [17].

As far as we know, there has been no research on humanoid robot where we first analyze multiple sets of motion capture data and apply the extracted feature to the biped gait generation.

III. HUMAN MOTION CAPTURE AND WALKING PATTERN GENERATION

A. Experimental Condition

As shown in the right side of Fig.1, we captured the human walking motion. We asked a woman with 1.67 [m] tall to walk straight ahead. We attached 86 markers to her whole body and captured the walking motion. As shown in Table I, we captured 9 sets of walking motion for different target step length and different target cycle time. In this research, we focus on the motion of the lower body of the human and consider applying the feature of human motion to humanoid robots. For this purpose, we calculated the motion of the waist and the foot for each captured human walking data.

The feature of the human walking data is extracted and will be applied to the biped humanoid robot. Fig. 2 shows the

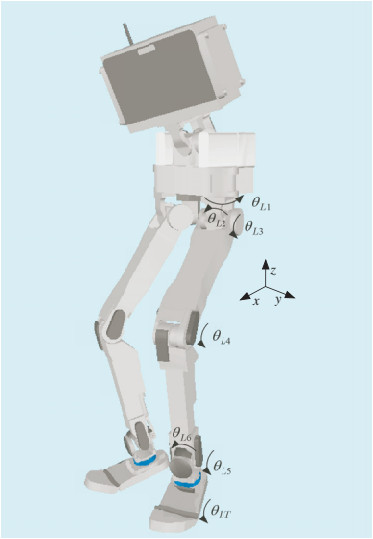

Fig. 2. Leg Module of HRP-4

overview of the biped walking robot used in this research. This robot has 6 joints between the waist and the foot. In addition, this robot has a toe joint in each foot. Also, this robot has 3 DOF waist joint. Since the length of this robot's leg is almost same as the human's one, the extracted feature of the human motion is directly applied to this robot without changing the scale of the motion.

Now, let us explain how to generate the walking motion of the robot. While we focus on the motion of a humanoid robot within the sagittal $(x-z)$ plane, the motion in the frontal $(y-z)$ plane can also be treated in the same fashion. Let us assume that the ZMP trajectory of a humanoid robot is given by a spline function. Let $\boldsymbol{p}_{zmp}^{(j)} = [x_{zmp}^{(j)}\ y_{zmp}^{(j)}\ z_{zmp}^{(j)}]^T$ be the trajectory of the ZMP belonging to the j-th segment of time. The trajectory of ZMP in the sagittal plane can be expressed as:

$$x_{zmp}^{(j)} = \sum_{i=0}^{n} a_i^{(j)}(t-t_{j-1})^i, \quad t_{j-1} \le t \le t_j, \quad j = 1, \cdots, m \tag{1}$$

where $a_i^{(j)}$ $(i = 0, \cdots, n,\ j = 1, \cdots, m)$ are scalar coefficients. An example of the ZMP trajectory is shown in Fig.3.

Let $\boldsymbol{p}_G^{(j)} = [x_G^{(j)}\ y_G^{(j)}\ z_G^{(j)}]^T$ be the trajectory of the COG(Center of Gravity) corresponding to the ZMP trajectory belonging to the j-th segment of time. Also, let $\mathcal{L}^{(j)} = [\mathcal{L}_x^{(j)}\ \mathcal{L}_y^{(j)}\ \mathcal{L}_z^{(j)}]^T$ be the angular momentum of the robot about the COG. The relationship between the ZMP and the COG within the sagittal plane is expressed by the following ordinary differential equation:

$$x_{zmp}^{(j)} = \frac{-\dot{\mathcal{L}}_y^{(j)} + M x_G^{(j)}(\ddot{z}_G^{(j)} + g) - M(z_G^{(j)} - z_{zmp}^{(j)})\ddot{x}_G^{(j)}}{M(\ddot{z}_G^{(j)} + g)}. \tag{2}$$

Let $z_{Go}^{(j)}$ be the initial value of $z_G^{(j)}$ and be $x_G^{(j)} = \bar{x}_G^{(j)} + \Delta x_G^{(j)}$. Eq.(2) can be split into the following two equations:

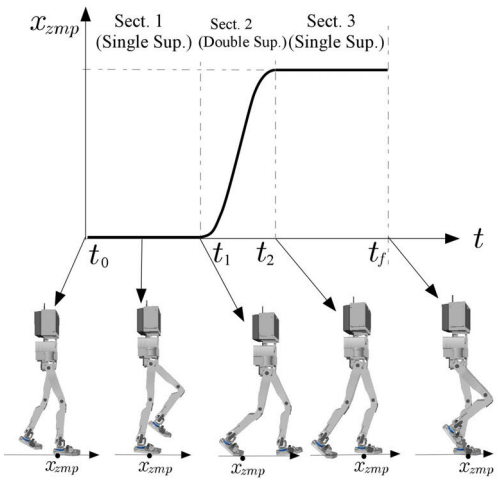

Fig. 3. ZMP Trajectory

$$x_{zmp}^{(j)} = \bar{x}_G^{(j)} - \frac{z_{Go}^{(j)} - z_{zmp}^{(j)}}{g}\ddot{\bar{x}}_G^{(j)} \quad (3)$$

$$f_x = \Delta x_G^{(j)} - \frac{z_{Go}^{(j)} - z_{zmp}^{(j)}}{g}\Delta\ddot{x}_G^{(j)} \quad (4)$$

where

$$f_x = \frac{\dot{\mathcal{L}}_y^{(j)}}{M(\ddot{z}_G^{(j)} + g)} - \left(\frac{z_{Go}^{(j)} - z_{zmp}^{(j)}}{g} - \frac{z_G^{(j)} - z_{zmp}^{(j)}}{\ddot{z}_G + g}\right)\ddot{x}_G. \quad (5)$$

Substituting eq.(1) into eq.(3) and solving with respect to $\bar{x}_G^{(j)}$, we obtain the analytical solution of the nominal position of the COG as

$$\bar{x}_G^{(j)} = V^{(j)}\cosh(w_c(t - t_{j-1})) + W^{(j)}\sinh(w_c(t - t_{j-1})) + \sum_{i=0}^{n} A_i^{(j)}(t - t_{j-1})^i, \quad j = 1, \cdots, m \quad (6)$$

$$a_i^{(j)} = A_i^{(j)} - \frac{1}{T_c^2}(i+1)(i+2)A_{i+2}, \quad i = 0, \cdots, n-2 \quad (7)$$

$$a_i^{(j)} = A_i^{(j)}, \quad i = n-1, n \quad (8)$$

where $w_c = \sqrt{g/(z_G - z_{zmp})}$, and $V^{(j)}$ and $W^{(j)}$ $(j = 1, \cdots, m)$ denote the scalar coefficients. Although, in [24], we propose the real-time gait generation method, we use the same method for the off-line walking pattern generation in this research. In most of the cases, although $\Delta x_G^{(j)}$ is much smaller than $\bar{x}_G$, we show later of this paper that $\Delta x_G^{(j)}$ is important in realizing the human-like motion. $\Delta x_G^{(j)}$ is calculated by using the dynamics filter based on the preview control [16].

IV. ANALYSIS OF CAPTURED MOTION

In this section, we consider analyzing the human-motion captured data and obtaining the parameters used for the walking pattern generator.

A. Experimental Condition

Fig.4 shows the definition of the physical quantities obtained by using the motion capture data. In this research, we focus on the motion of the lower body of the human. Assuming that each leg of the robot has 6 + 1 (toe) joints, the motion of the humanoid robot's lower body can be completely specified if we can specify the 6 dimensional motion of the waist and the both feet and the joint motion of the toe.

First, we analyze the motion capture data. If the vertical velocity of both feet is smaller than the predefined threshold, we define the double support phase around this period of time. Then, we obtain the time at the middle of the double support phase. Let t_{fk} be the time at the middle of the k-th double support phase. We define $T_k = t_{fk} - t_{f,k-1}$ as the cycle time of the k-th step. Also, let us focus on the motion of the foot in the sagittal plane. We define the motion of the foot at the rotation center of the ankle joint. Let $x_{f,k-1}$ be the horizontal position of the foot going to lift off in the $k-1$-th double support phase. Also, let x_{fk} be the position of the foot having touched to the ground in the k-th double support phase. We define $L_k = x_{fk} - x_{f,k-1}$ as the step length of the k-th step.

Among the six dimensional motion of the waist, the horizontal $(x - y)$ motion is determined by solving the differential equation for the given ZMP trajectory. Also, we found that the roll and the pitch rotation is smaller than the yaw rotation. Thus, in this section, we focus on the vertical (z) motion and the yaw rotation of the waist based on the motion capture data. Here, the horizontal motion of the waist will be considered in the next section. With regard to the motion of the foot, since we consider the human motion walking straight ahead, the roll and the yaw rotation of the foot is much smaller than the pitch rotation. Thus, we focus on the $x - z$ motion and the pitch rotation of the foot.

B. Vertical Motion of Waist

We first consider the vertical motion of the waist. Vertical position of the waist becomes maximum at the single support phase and becomes minimum at the double support phase. Let us consider the k-th step. As shown in Fig. 4, let the difference between the maximum and the minimum vertical position of the waist be ζ_k. Fig.5 show the result of the human motion capture. As far as we tried, there is no remarkable relationship between the cycle time and ζ_k. On the other hand, although it is not remarkable too, we can recognize that ζ_k increases as the step length increases. The line shown in the right figure expresses the 2nd order curve fitted by using the least squares method. This curve is calculated as

$$\zeta_k = 0.0019 - 0.0015L_k + 0.01L_k^2 \quad (9)$$

We applied this ζ_k when generating the walking pattern of a humanoid robot.

There are several researches on humanoid biped gait considering the vertical motion of the waist. However, in most of the human-sized humanoid robot, the length of the

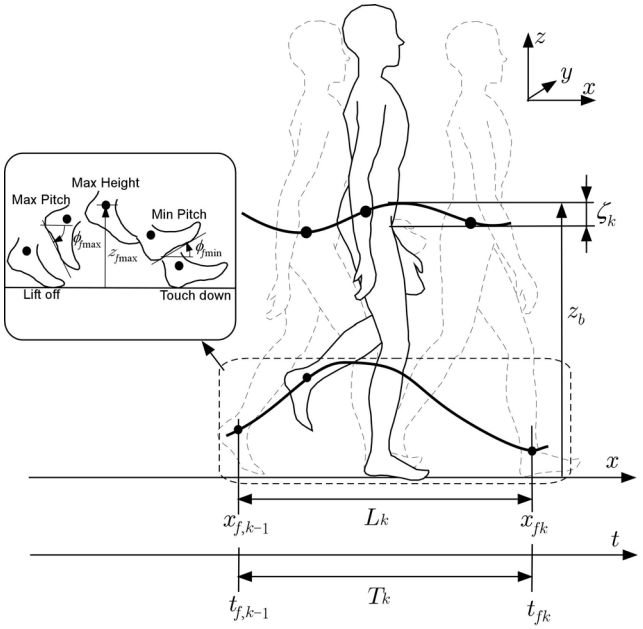

Fig. 4. Definition of Parameters used to Analyze the Motion Capture Data

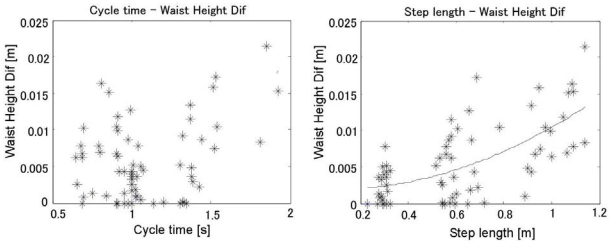

Fig. 5. Difference of Waist Height of Human Motion Capture

step is less than 0.4 [m]. Our experiment indicates that the vertical motion of the humanoid robot's waist is less than 10 [mm] and is very small. On the other hand, the step length of the human's gait often exceeds 1 [m]. In this case, the vertical motion of the waist becomes more significant.

C. Yaw Motion of Waist

Fig. 6 shows the plot of the yaw rotation of the human's waist. The top figure shows the plot of $r_{yk} = (t_{ymax} - t_{f,k-1})/T_k$ as a function of the cycle time where t_{ymax} denotes the time when the yaw rotation becomes maximum. As shown in this figure, the yaw rotation becomes maximum at the middle of the double support phase regardless of the cycle time. Hence, we set $r_{yk} = 1$ when generating the walking pattern of a humanoid robot. The bottom left figure shows the maximum yaw rotation as a function of the cycle time. There is no significant relationship between the cycle time and the yaw rotation. On the other hand, the bottom right figure shows the maximum yaw rotation as a function of the step length. As we can see from this figure, the maximum yaw rotation increases as the step length increases. The curved line in this figure shows the 2nd order curve fitted by using the least squares method. We applied this curve when generating the walking motion by a humanoid robot:

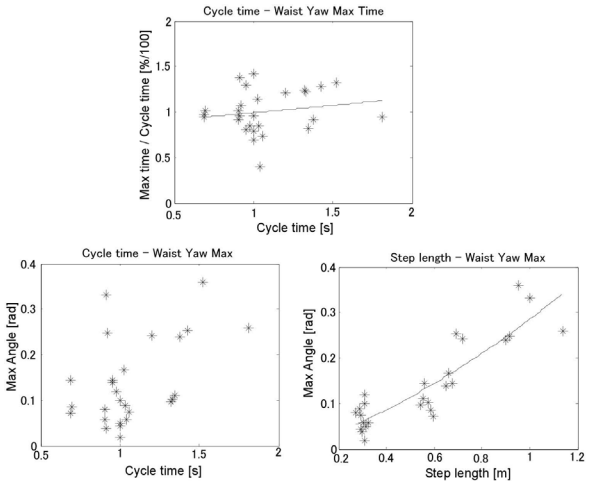

Fig. 6. Maximum Waist Yaw of Human Motion Capture

$$\phi_{yk} = 0.1835L_k + 0.157L_k^2 \tag{10}$$

When the humanoid robot walks with large step length, the leg often falls in the singular posture. The yaw rotation of the waist is effective in avoiding the leg to be in the singular posture. On the other hand, when the robot walks with small step length, the yaw rotation is not needed. By using our method, since the yaw rotation can be obtained as a function of the step length, it is effective in avoiding the leg to be in singular posture when the step length is large.

D. Swing Leg Motion

The left of the Fig.4 shows the motion of the swing foot. As shown in this figure, the pitch rotation becomes maximum after the foot lifts off. Then, the foot touches the ground after the pitch angle becomes minimum.

Fig.7 shows the plot of the ankle height. The top left of Fig.7 shows $r_{ak} = (t_{amax} - t_{f,k-1})/T_k$ as a function of the cycle time where t_{amax} denotes the time when the ankle height becomes maximum. As shown in this figure, the height of the ankle becomes maximum almost at the middle of the single support phase while this time slightly increases as the cycle time increases. The top right figure shows the plot of $\xi_{ak} = (x_{amax} - x_{f,k-1})/L_k$ where x_{amax} denotes the x coorinate of the ankle position maximizing its height. The ankle height becomes maximum almost at $\xi_{ak} = 0.4$. The bottom figure shows the maximum ankle height as a function of the step length. We can see from this figure that the ankle height slightly increase as the step length increases.

In our walking pattern generator, we fixed $r_{ak} = 0.5$ and applied the 2nd order curve of the maximum ankle height as a function of the step length fitted by using the least square method.

Figs.8 and 9 show the plot of the maximum and minimum pitch rotation of the foot, respectively. As shown in these figures, the time and x coordinate when the pitch rotation becomes maximum/minimum are almost constant regardless of the cycle time and the step length, respectively. On

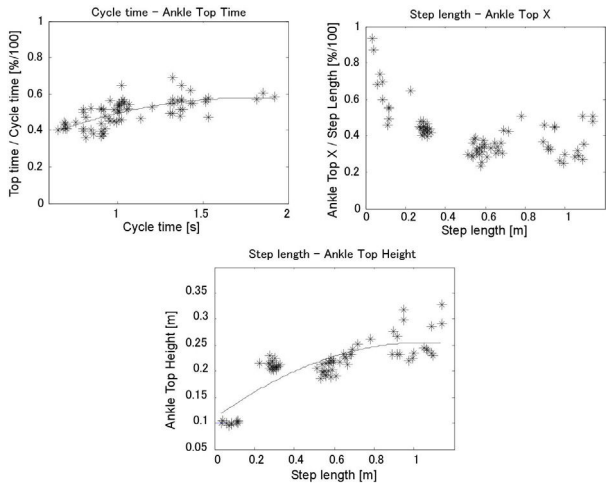

Fig. 7. Maximum Ankle Height of Human Motion Capture

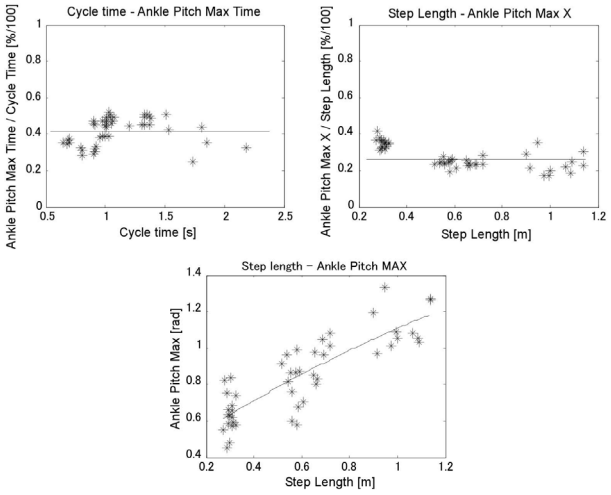

Fig. 8. Maximum Ankle Pitch of Human Motion Capture

the other hand, the maximum and minimum pitch rotation angle increases and decreases, respectively, as the step length increases.

In our walking pattern generator, we fixed the time when the pitch rotation becomes maximum/minimum and applied the 2nd order curve of the maximum/minimum pitch rotation angle as a function of the step length fitted by using the least square method.

V. HORIZONTAL MOTION OF WAIST

Next, we focus on the horizontal motion of the waist. Fig.10 shows the motion of the CoG within the lateral plane as a function of time. These figures compare the CoG trajectory between a human and a humanoid robot. Fig.10(a) shows $\bar{y}_G$ obtained by using eq.(6) where the step length and the cycle time are 0.3[m] and 1.25 [s], respectively. On the other hand, Fig.10(b) shows the human motion shown in the 3rd sample of Table I. We can see from these figures that the sway of the humanoid robot's waist is much larger than the human's one.

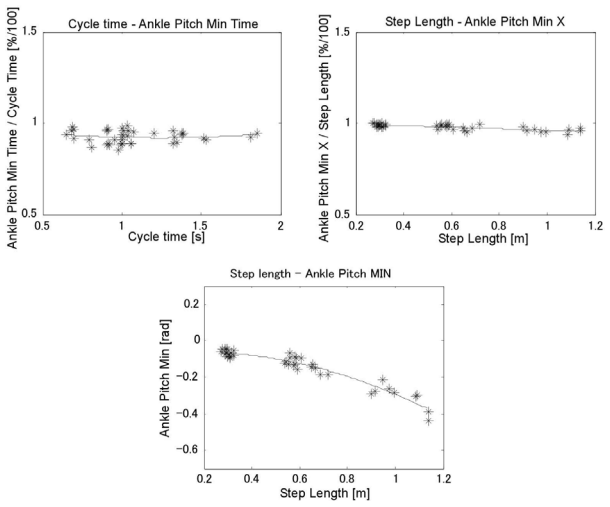

Fig. 9. Minimum Ankle Pitch of Human Motion Capture

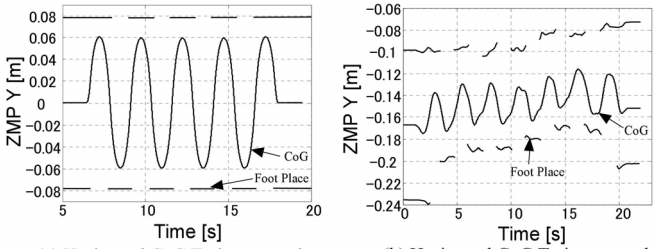

(a) Horizontal CoG Trajectory and Foot Place of a Humanoid Robot

(b) Horizontal CoG Trajectory and Foot Place of a Human

Fig. 10. Horizontal CoG Trajectory of Humanoid Robot and Human

We consider two effects to reduce the sway of the humanoid robot's waist. One is to take Δy_G in eq.(4) into account and the other is to make the robot's ZMP trajectory in the single support phase be close to the human's one. The ZMP trajectory in the single support phase is shown in Fig.11. As shown in this figure, the human's ZMP moves to the toe at the middle of the single support phase. We also make the robot's ZMP move during the single support phase. The motion of the ZMP in the x direction contributes to avoid the knee of the stance foot fall in the singular posture. On the other hand, the motion of the ZMP in the y direction contributes to reduce the waist's sway.

Fig.12 shows the results of the reduction of the waist's sway where we set $x_{zt} = 0.04$, $x_{zh} = -0.005$, and $y_{zh} = 0.01$ [m]. Here, as shown in eq.(5), Δy_G compensates the effect of angular momentum and the vertical motion of the waist. Here, as shown in Fig.13, although we set the magnitude of waist's vertical motion about 0.01 [m], the effect of the waist's vertical motion is much smaller than that of the angular momentum.

VI. IMPLEMENTATION ISSUE

We installed the function explained in the previous section to the walking pattern generator. This section explains some implementation issues about our proposed method.

First, we did not explicitly give the initial vertical position of the waist. If the initial position of the waist is too high, it

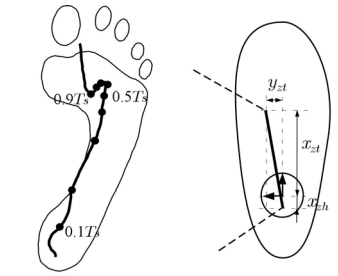

(a) ZMP Trajectory of a Human[20]

(b) ZMP Trajectory of a Humanoid Robot

Fig. 11. ZMP Trajectory of Humanoid Robot and Human

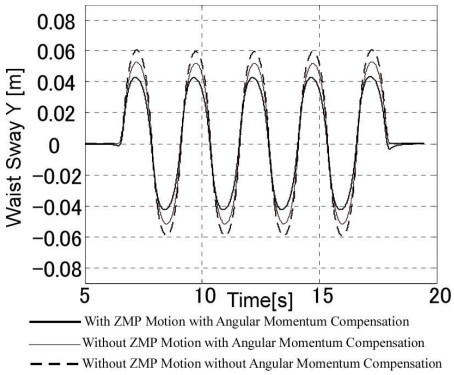

Fig. 12. Reduction of the sway of waist

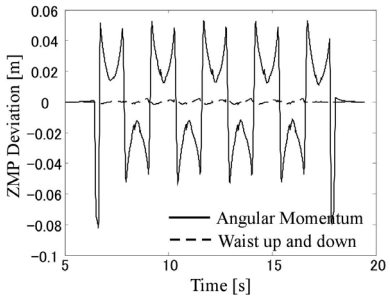

Fig. 13. Effect of Angular Momentum and Vertical Waist Motion on ZMP Deviation

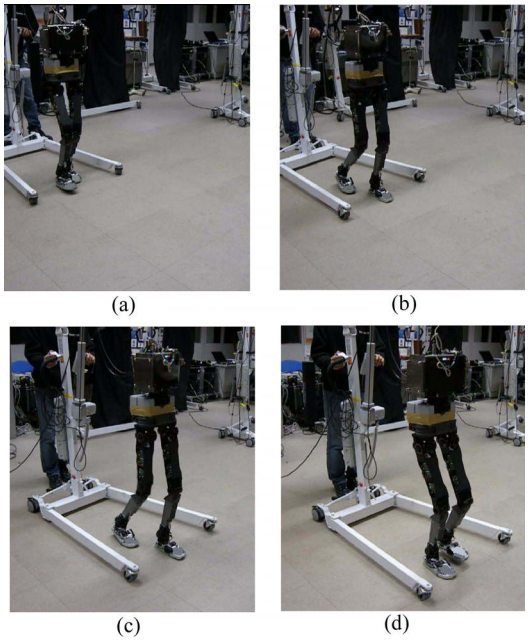

Fig. 15. Experimental Result

sometimes become impossible to place the foot to the desired position. Thus, we first give the initial vertical position of the waist and check the joint velocity of the legs during the walking motion. If the velocity is too large, we make the initial position lower than the first trial. Otherwise, we make the initial position higher than the first trial. We iterate this operation until the initial waist position becomes high enough and joint velocity is within the predefined limit.

Second, a human usually lifts his/her heel during the single support phase. This contributes to enlarge the step length. On the other hand, in our walking pattern generator, the heel always touch the ground during the single support phase. In this case, when the step length is large, we have to make the vertical position of the waist lower at the beginning of the double support phase. Hence, we modified eq.(9) as follows:

$$\zeta_{k+1} = 0.002 + 0.144L_k^2 \tag{11}$$

By using this equation, the magnitude of up/down of the waist becomes 0.015 [m] when the step length is $L_k = 0.3$[m].

Thirdly, as shown in Fig.11, the human's zmp trajectory during the single support phase moves close to the thumb finger. Learned from this characteristic, we set $y_{zt} = 0.01$[m] in Fig. 12 and the sway of the waist could be reduced. However, the foot of our humanoid robot is connected to the ankle joint through the rubber bush. In this case, if we set $y_{zt} = 0.01$[m], unexpected bend of the rubber is introduced and the swing leg touches the ground earlier than expected. Thus, in simulation and experiment shown in the next section, we set $y_{zt} = 0.0$[m].

VII. RESULTS

We performed simulation and experiment by using the leg module of HRP-4. We basically used the walking pattern generator proposed in [25] and wrapped our proposed method explained in this paper. Fig.14 shows the simulation result. In this simulation, we set the step length as $L_1 = 0.15$, $L_2 = 0.3$, $L_3 = 0.3$, $L_3 = 0.3$, and $L_4 = 0.15$ [m]. In this simulation, the robot changes the pitch angle of the foot, height of the foot, up/down of the waist, and yaw rotation of the waist depending on the step length. Also, Fig.15 shows the experimental result. We can see that the robot can stably walk without falling down. Here, we have deleted the foot mechanism from these figures due to the patent problem.

VIII. CONCLUSIONS AND FUTURE WORKS

In this paper, we generated a biped gait of a humanoid robot based on the human motion capture data. We first analyze a set of human motion capture data and extracted the information needed to generate the gait pattern of a humanoid

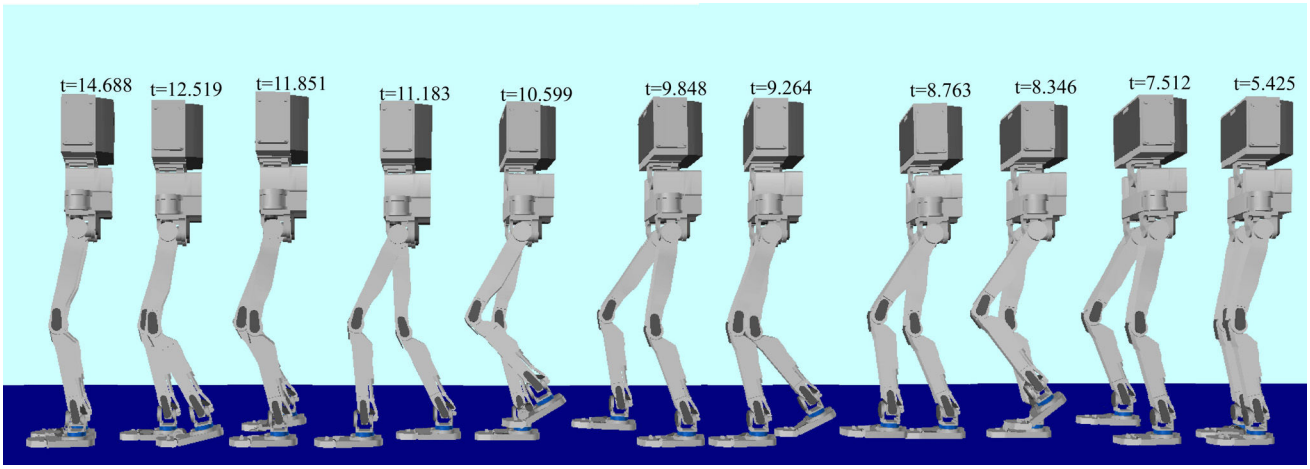

Fig. 14. Simulation Result

robot. In our gait generation method, the up/down of the waist, the yaw rotation of the waist, and the ankle rotation are the function of the step length and the gait cycle time. Also, we show how to reduce the sway of the waist. The effectiveness of the proposed approach was confirmed by simulation and experimental results.

We have a lot of future works to realize the human like gait in several situations. First, we will automatically determine the initial height of the waist. Then, we consider realizing the turning motion. Also, we will consider the effect of y_{zt} for the simulation and experiments. Also, we will increase the number of subjects capturing the walking motion.

REFERENCES

[1] S. Nakaoka, A. Nakazawa, K. Yokoi, H. Hirukawa, and K. Ikeuchi: "*Generating Whole Body Motions for a Biped Humanoid Robot from Captured Human Dances*", Proc. of 2003 IEEE Int. Conf. on Robotics and Automation, 2003.

[2] N. S. Pollard, J. K. Hodgins, M. J. Riley, and C. G. Atkeson: "*Adapting human motion for the control of a humanoid robot*", Proc. of 2002 IEEE Int. Conf. on Robotics and Automation, 2002.

[3] L. Ren, A. Patrick, A.A. Efros, J.K. Hodgins, and J.Rehg: "*A Data-Driven Approach to Quantifying Natural Human Motion*", ACM Transactions on Graphics, Vol. 24, No. 3, 2005.

[4] O. Arikan and D.A. Forsyth: "*Interactive Motion Generation from Examples*", ACM Transactions on Graphics, Vol. 21, No. 3, 2002.

[5] M. Gleicher: "*Comparing Constraint-based Motion Editing Methods*", Graphical Models, vol. 63, no. 2, pp. 107-134, 2001.

[6] L. Ikemoto and D.A. Forsyth: "*Enriching a Motion Collection by Transplanning Limbs*", Proc. of 2004 ACM SIGGRAPH/Eurographics Symp. on Computer Animation, pp. 99-108, 2004.

[7] W. Suleiman, E. Yoshida, F. Kanehiro, J-P. Laumond, and A. Monin: "*On Human Motion Imitation by Humanoid Robot*", Proc. of 2008 IEEE Int. Conf. on Robotics and Automation, 2008.

[8] T. Flash and N. Hogan: "*The Coordination of Arm Movements: An Experimentally Confirmed Mathematical Model*", J. Neuroscience, vol. 5, no. 7, pp. 1688-1703, 1985.

[9] Y.Uno, M.Kawato, and R.Suzuki: "*Formation and Control of Optimal Trajectory in Human Multijoint Arm Movement Minimum Torque-Change Model*", Biological Cybernetics, no. 61, pp. 89-101, 1989.

[10] M.Svinin, Y.Masui, Z.-W.Luo, and S.Hosoe: "*On the Dynamic Version of the Minimum Hand Jerk Criterion*", J. of Robotic Systems, vol. 22, no. 11, pp. 661-676, 2005.

[11] J.E.Bobrow, B.Martin, G.Sohl, E.C.Wang, F.C.Park, and J.Kim: "*Optimal Robot Motions for Physical Criteria*", J. Robotic Systems, vol. 18, no. 12, pp. 785-795, Dec 2001.

[12] M.B. Popovic, A. Goswami, and H. Hurr: "*Ground Reference Points in Legged Locomotion: Definitions, Biological Trajectories and Control Implications*", Int. J. of Robotics Research, vol. 24, no. 12, pp. 1013-1032, 2005.

[13] K. Hirai, M. Hirose, Y. Haikawa, T. Takenaka: "The Development of Honda Humanoid Robot", Proc. of 1998 IEEE Int. Conf. on Robotics and Automation, pp. 1321-1326, 1998.

[14] M.Fujita, Y.Kuroki, T.Ishida, and T.Doi: "Autonomous Behavior Control Architecture of Entertainment Humanoid Robot SDR-4X", Proc. of IEEE/RSJ Int. Conf. Intelligent Robots and Systems, pp. 960-967, 2003.

[15] K. Kaneko et al.: "*The Humanoid Robot HRP2*", Proc. of IEEE Int. Conf. on Robotics and Automation, 2004.

[16] S.Kajita et al.: "*Resolved Momentum Control*", Proc. of 2003 IEEE/RSJ Int. Conf. on Intelligent Robots and Systems, 2003.

[17] L. Sentis and O. Khatib,: "*Synthesis of whole-body behaviors through hierarchical control of behavioral primitive*", Int. J. of Humanoid Robotics, 2005.

[18] K. Hauser, T. Bretl, and J.-C. Latombe: "*Non-Gaited Humanoid Locomotion Planning*", Proc. of IEEE-RAS/RSJ Int. Conf. on Humanoid Robotics, 2005.

[19] T. Bretl, S.Lall, J.-C. Latombe, and S.Rock: "*Multi-step Motion Planning for Free-climbing Robots*", Proc. of 6th Int. Workshop on Algorithmic Foundation of Robotics(WAFR), 2004.

[20] Y. Ebara and S. Yamamoto: "*Introduction of Body Dynamics –Analysis of Gait and Gait Initiation–*", Ishiyaku Publishers Inc., 2002 (in Japanese).

[21] T. Bretl: "*Motion Planning of Multi-Limbed Robots Subject to Equilibrium Constraints: The Free-Climbing Robot Problem*", To appear in Int. J. Rob. Res., 2006.

[22] J.J. Kuffner, Jr., K. Nishiwaki, S. Kagami, M. Inaba, H. Inoue,: "Motion Planning for Humanoid Robots", Int. Symp. Rob. Res., 2003.

[23] H. Choset, K.M. Lynch, S. Hutchinson, G. Kanto, W. Burgard, L.E. Kavraki, and S. Thrun: "Principles of Robot Motion: Theory, Algorithms, and Implementations", MIT Press,2005.

[24] K.Harada, S.Kajita, K.Kaneko, and H.Hirukawa: "*Analytical Method on Real Time Gait Planning for a Humanoid Robot*", Proc. of 2004 IEEE-RAS/RSJ Int. Conf. on Humanoid Robotics, 2004.

[25] S. Kajita, F. Kanehiro, K. Kaneko, K. Fujiwara, K. Harada, K. Yokoi, and H. Hirukawa, Biped Walking Pattern Generation by using Preview Control of Zero-Moment Point, *Proc. of IEEE Int. Conf. on Robotics and Automation*, pp. 1620-1626, 2003.